Role of Hydrophobic Clusters in the Stability of α-Helical Coiled Coils and Their Conversion to Amyloid-like β-Sheets

He Dong and Jeffrey D. Hartgerink*

Departments of Chemistry and Bioengineering, Rice University, 6100 Main Street MS60, Houston, Texas 77005

Received September 13, 2006; Revised Manuscript Received November 1, 2006

We designed a library of short peptides using standard rules for coiled-coil assembly. Depending on the composition of amino acids in the non-interacting region of the coiled coil (positions b, c, and f) these peptides are able to convert from α-helical to β-sheet secondary structure. This type of transition is observed in amyloid-like proteins and is a key feature associated with many types of neurodegenerative diseases. Studies on peptides that are 14 amino acids in length indicated that positioning hydrophobic amino acids at an f position within a heptad repeat accelerated the rate of conformational conversion as compared to that at a c position. We believe that this occurs because of the formation of a hydrophobic pocket that preferentially stabilizes β-sheets over α-helices. This effect was also observed in longer 21 amino acid peptides. Our study shows that the relative rates of structural conversion correlate with the formation of a continuous three-amino-acid hydrophobic patch consisting of amino acids in the d, f, and a positions and not on the secondary structure propensities of the individual amino acids. The sequence−structure relationship observed in this study will be used to help understand the mechanism of amyloid fiber formation and design future coiled-coil and β-sheet-forming peptide systems.

Introduction

Both the assembly of α-helical coiled coils and β-sheet amyloids are in large part driven by the packing of hydrophobic amino acids to form their characteristic structure. Coiled coils are formed by the packing of two (or more) α-helices against one another.[1] This packing is driven to bury the exposed hydrophobic face of each helix at the interface of the two peptides and reinforces the intramolecular backbone hydrogen-bonding network of both α-helices. In coiled-coil design a seven-amino-acid repeat (a "heptad" whose amino acids can be labeled a−g) is found in which amino acids in the a and d positions are hydrophobic and typically leucine, isoleucine, or valine.[2,3] Because seven amino acids make approximately two turns of an α-helix, the a and d positions align along one face of the α-helix making it highly hydrophobic (Figures 1a and 1b). Amyloid-like β-sheets are also facial amphiphiles but achieve their amphiphilic nature by a simple alternation of hydrophobic and hydrophilic amino acids, which, in a fully extended conformation, leads to one face of the peptide being hydrophobic and one being hydrophilic.[4−9] Similar to the coiled-coil structure, the hydrophobic packing reinforces the hydrogen-bonding network, although here the hydrogen bonds are intermolecular as opposed to intramolecular.[10] If a coiled-coil sequence is mapped to an extended conformation, then one sees that it does not match the necessary requirements for amyloid-like β-sheet formation. Likewise an alternating hydrophobic/hydrophilic sequence mapped to an α-helix does not satisfy the requirements for a coiled coil.

The specific pattern of hydrophobic and hydrophilic residues in the sequence allows one to design a protein with predetermined secondary structure. Early examples include the work done by DeGrado,[11] which focused on the formation of static secondary structures (e.g., random coil, α-helix, and β-sheet) by changing the order of the residues on model peptides so as to create hydrophobic repeating units that favor certain types of protein secondary structure. Later, others also reported on systems where the conformations of designed peptides can be controlled by changing the solvent medium,[12] redox states of the residues,[13,14] pH,[9] peptide chain length,[15] and the addition of metal ions[16,17] based on the same idea of patterning hydrophobic and hydrophilic residues periodically to stabilize one type of secondary structure. It is worth emphasizing that the peptides mentioned above adopt one specific stable conformatio, unless the solvent or other environmental factors are changed. Recently, Mihara's group developed a series of peptides that showed structural conversion from α-helix to β-sheet.[18−21] The transition between the two conformations is self-initiated and without the need for an environmental trigger (although elevated temperature may accelerate the process of structural conversion). However, these peptides were modified by hydrophobic "defects" mostly consisting of non-amino-acid components at the N-termini. Some studies[9,15−23] have shown that, by rational design, one can manipulate peptide conformations as well as structural transition.[22,23] The structural transition, specifically, from α-helix to β-sheet is associated with many types of neurodegenerative diseases and has attracted attention from both theoretical and experimental perspectives.[24,25] In this paper, we design a peptide system that exhibits dynamic formation of secondary structures mimicking the natural disease-related peptide (amyloid-beta peptide). This work helps to elucidate the mechanisms of structural polymorphism in amyloid-forming proteins and should help to guide the design of both coiled-coil and β-sheet peptide architectures.

Recently we have investigated the minimum length necessary to form a stable coiled coil. In that study, a 14-amino-acid peptide (peptide **1**) was found to form a dimeric coiled coil at 5 °C, but at elevated temperatures the α-helical structure converts to amyloid-like, antiparallel β-sheet nanofibers.[26] This led us in this study to formulate a generalized rationale for such

* Author to whom correspondence should be addressed. Phone: (713) 348-4142. E-mail: jdh@rice.edu.

10.1021/bm060871m CCC: $37.00
Published on Web 01/18/2007

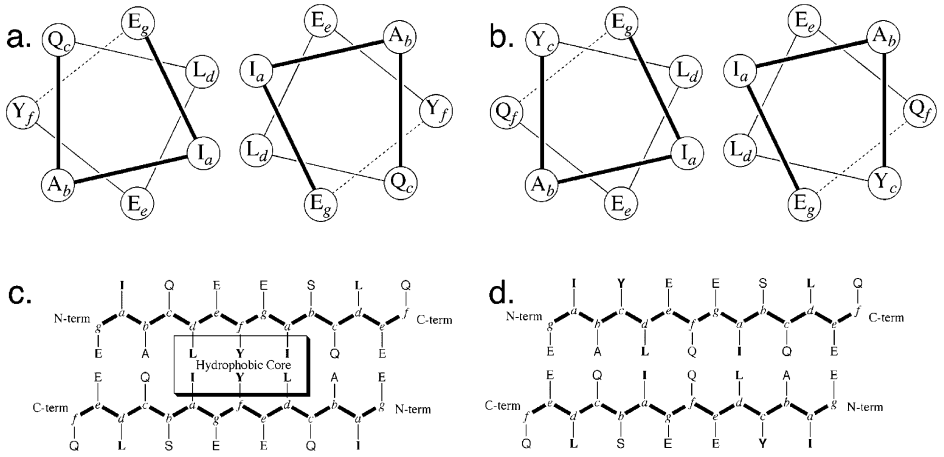

Figure 1. Structural arrangement of peptides **1** (a and c) and **3** (b and d) in the coiled-coil or amyloid-like β-sheet packing motifs. Amino acids are represented with the standard, upper-case, single-letter code while the position in the heptad repeat is indicated in lower-case italics. In all cases the hydrogen-bonding network is formed normal to the figure. Similar comparisons can be made for the larger three-heptad peptides **5** and **6**.

Table 1. Peptide Primary Sequences Studied in This Paper

	sequence[a]
peptide no.	*gabcdefgabcdefgabcdef*
1	EIAQLEYEISQLEQ[b]
2	EIAQLESEISQLEQ
3	EIAYLEQEISQLEQ
4	EIAQLEYEISQLEQEIQALES[b]
5	EIAQLEYEISQLEYEIQALES
6	EIAYLEQEISYLEQEIQALES
7	EIAQLEFEISQLEFEIQALES
8	EIAQLELEISQLELEIQALES

[a] The N- and C-termini of all peptides are acetylated and amidated, respectively. [b] The initial description of these peptides is in ref 26.

structural instability by the examination of 8 peptides of different sequences containing 14 or 21 amino acids. Our hypothesis is that positioning a hydrophobic amino acid in the f position of a heptad repeat leads to the formation of a continuous hydrophobic patch composed of the amino acids in positions d, f, and a, which all lie on one side of the peptide when the peptide is in a fully extended conformation (Figure 1c). Two such peptides can then pack against one another in an extended conformation, burying the hydrophobic patch to form the nucleus for a β-sheet hydrogen-bonded structure.

To test this hypothesis, we prepared two sets of peptides with a general coiled-coil motif. The first set is only 14 amino acids (two heptads) in length while the second set is 21 amino acids (three heptads) in length (Table 1). The general design incorporates Ile and Leu in the a and d positions, respectively, and hydrophilic or α-helix-inducing amino acids in the b, c, and f positions. The e and g positions are filled with glutamic acid to allow pH-controlled assembly and disassembly of the peptides depending on the charge of the carboxylic acid. On the basis of these design criteria, derivatives were prepared to test the importance of a dfa hydrophobic patch in which amino acids in the f position incorporate Ser, Gln, Tyr, Phe, or Leu.

Peptide **1**[26] incorporates a dfa hydrophobic patch. It is a stable dimeric coiled coil when the pH is below 5 and at 5 °C. At room temperature this peptide slowly converts to an amyloid-like β-sheet nanofiber. The nanofibers reveal green-yellow birefringence in the presence of congo red dye and are approximately 5 nm in diameter and hundreds of nanometers in length as revealed by transmission electron microscopy (TEM). The structural transition is highly temperature-dependent and takes place following autocatalytic kinetics. Circular dichroism (CD) after an appropriate amount of time or after mild heating reveals a β-sheet signature characterized by a minimum at 216 nm. Specifically, the α-helical structure of peptide **1** converts to β-sheet in 30 min at 50 °C (Table 2). Fourier transform infrared (FT-IR) spectroscopy of a dried film confirms this structural transition with a shift of the amide I band from 1654 to 1623 and 1611 cm^{-1}. A weak shoulder at 1692 cm^{-1} suggests that the β-sheet structure being formed has a significant antiparallel component (Figure 2d).

Table 2. Comparison of Peptides' Initial Helicity and Rate of Structural Transition

peptide no.	percent helicity at 5 °C	temperature for transition to β-sheet	lag time/time to 50% transition at 50 °C
1	70	55	20.5/30 min
2	75	76	>300 min
3	68	69	167/174 min
4	90	*a*	*a*
5	62	53	2.5/4.4 min
6	71	*a*	*a*
7	66	43	1.5/2.5 min
8	66	49	0/4.0 min

[a] These peptides do not undergo an α-to-β transition but instead unfold.

Results

To test the idea that the dfa hydrophobic patch is responsible for the instability of the α-helical structure, peptide **2** was prepared in which tyrosine (in position f) was replaced with the hydrophilic amino acid serine. This substitution increases the observed helicity from 70% to 75% (Figure 2b, Table 2) and substantially inhibits the formation of the β-sheet structure. Although β-sheet structure can still be observed by FT-IR after boiling a solution and examining a dried film of this material, CD shows that the peptide does not undergo conversion within 300 min at 50 °C. At 70 °C the peptide is still weakly helical, and only at 90 °C do we begin to see signs of a weak β-sheet developing. This is evidence that the dfa hydrophobic patch is largely responsible for stabilizing the β-sheet structure. However, one may also suggest that overall hydrophobicity, or the higher

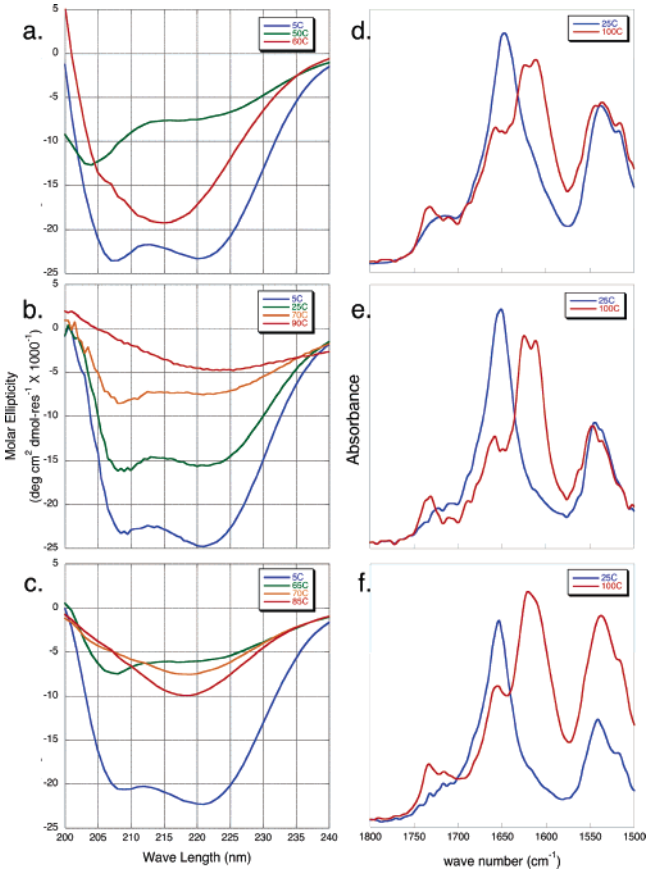

Figure 2. CD spectra of peptides **1**−**3** (a−c, respectively), at different temperatures. Concentration: 0.8 mg/mL. ATR FT-IR spectra of peptides **1**−**3** (d−f, respectively) before and after boiling. IR spectra were observed as dried films.

preference of serine for α-helix structure as compared to tyrosine, is more important than the specific positioning of the hydrophobic amino acids. To clarify this, peptide **3** was prepared in which instead of simply replacing tyrosine it is swapped with the glutamine occupying position c. Comparing peptide **1** to peptide **3**, we can see that the overall hydrophobicity and secondary structure preference should be identical since the amino acid composition is identical and only the order is different.

The CD spectrum of peptide **3** reveals similar helicity (Figure 2c, Table 2) compared to peptide **1** (68% vs 70%) but has a substantially greater resistance to β-sheet conversion. At 60 °C peptide **1** has β-sheet structure while peptide **3** is still helical (compare Figures 2a and 2c). The characteristic lag time before transition to β-sheet and the total time required for transition dramatically increase from peptide **1** to peptide **3** (Figure 3a, Table 2).

These three peptides might be considered unusual or not representative of coiled coils in general because of their very short length. The stability of α-helical structure is strongly dependent on the length of the helix since the four amino acids on each termini of the helix will only have half of their potential hydrogen bonds satisfied. This is in contrast to an amyloid-like β-sheet nanofiber in which all hydrogen bonds will be satisfied with the exception of the peptides at the very tips of the fibers which are in the extreme minority when the length of the fiber is on the order of hundreds of nanometers. To determine if structural transitions could be induced in longer coiled-coil peptides, five additional peptides, 21 amino acids (three heptads) in length, were studied.

Peptide **4**[26] incorporates the same general amino acid selection criteria used in the shorter peptides and has a single dfa

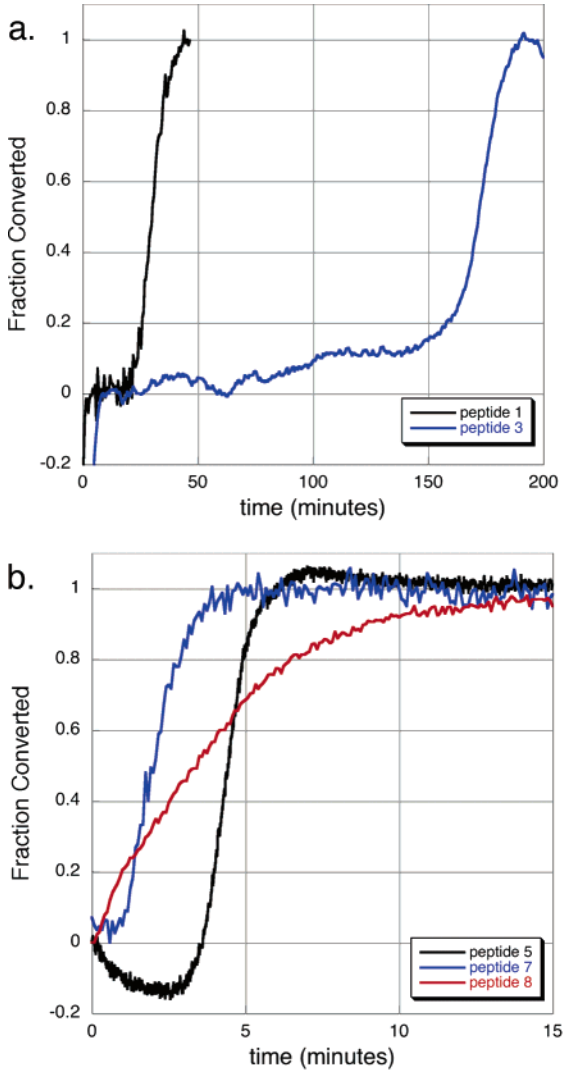

Figure 3. Change from α-helix to β-sheet monitoring at 205 nm and 50 °C. (a) Two-heptad peptides **1** and **3**. (b) Three-heptad peptides **5**, **7**, and **8**. Peptide **2** (not shown) does convert to β-sheet under these conditions but requires in excess of 5 h. Peptides **4** and **6** do not undergo helix-to-sheet transitions under the conditions tested.

hydrophobic patch between the first and second heptad. This peptide is highly helical as a coiled-coil dimer as indicated by the CD spectrum at 5 °C (90%, Table 2, Figure 4a). Heating the peptide results in simple unfolding rather than structural transition as indicated by the CD spectrum (Figure 4a). Even boiling the peptide and examining a dried film by attenuated total reflectance (ATR) FT-IR shows only major absorptions characteristic of an α-helix (1649 cm^{-1}, Figure 4f). A second dfa hydrophobic patch was incorporated between the second and the third heptad in peptide **5**. This peptide continues to show α-helical character at 5 °C by CD (62%), but the IR spectrum reveals that this peptide converts to a β-sheet structure upon heating by the presence of a strong peak at 1623 cm^{-1} with a significant antiparallel component as indicated by a secondary peak at 1693 cm^{-1} (Figure 4 g). The CD spectrum at 50 °C shows that the helical structure converts to β-sheet in only 4.4 min (Figure 3b). Peptide **5** was further analyzed by TEM to inspect the microscopic structure change upon heating. Two distinct structural morphologies were obtained as shown in Figures 5a and 5b and Figure 3 of the Supporting Information, with amorphous α-helical aggregates in the unheated solution and long β-sheet fibers present in the heated sample. As in the case of the two-heptad peptides, moving the hydrophobic amino

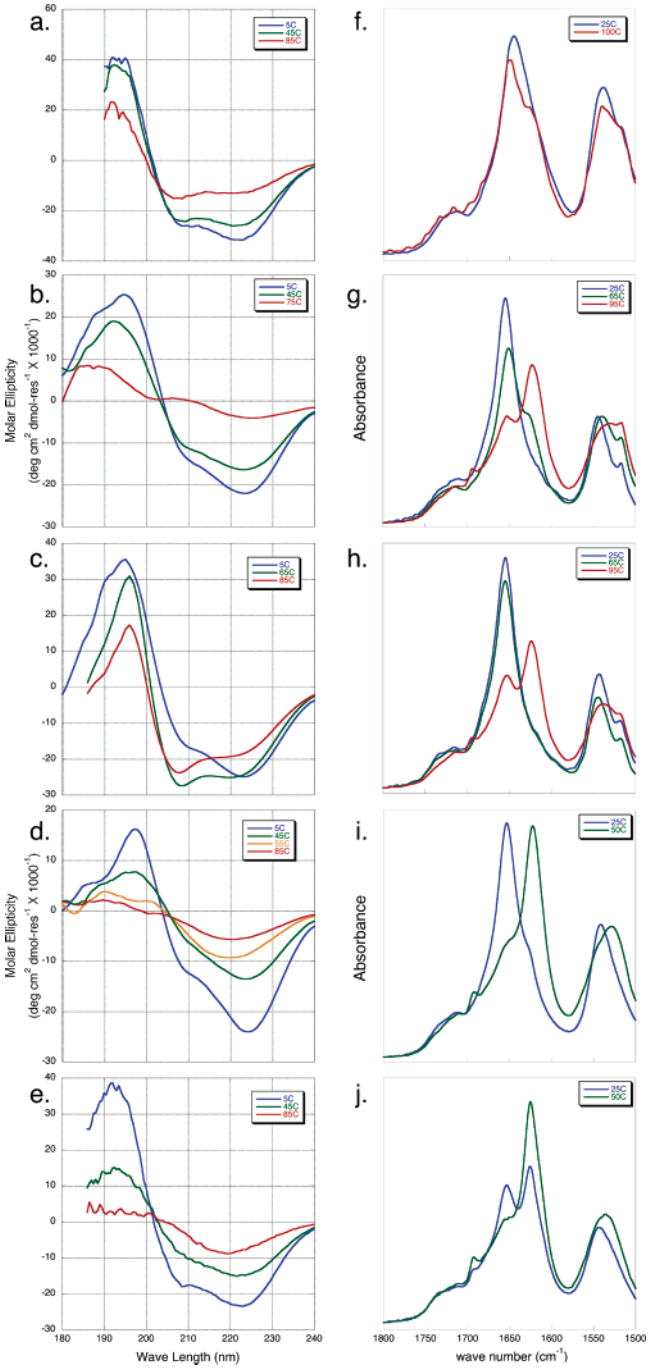

Figure 4. (a–e) CD spectra of peptides **4**–**8** (respectively) at 0.4 mg/mL and different temperatures. (f–j) FT-IR spectra of peptides **4**–**8** (respectively) before and after heating to the indicated temperatures and examined as dried films.

acid tyrosine to the c position strongly inhibits the transition to β-sheet. Peptide **6** (otherwise identical with peptide **5**, but with tyrosine swapped into the c positions and glutamine into the f positions in the first and second heptad repeat) does not convert to β-sheet at 50 °C as observed by CD. FT-IR experiments reveal that after heating to 65 °C the peptide is still entirely α-helical while peptide **5** contained a substantial population of β-sheet structure (compare Figures 4g and 4h). Only upon heating to 95 °C does peptide **6** show a similar population of antiparallel β-sheet conformation with absorbances at 1621 and 1693 cm^{-1}(Figure 4h).

To explore the orientation of these peptide backbones (and thus the hydrogen-bonding network) with respect to the fiber axis, we performed additional FT-IR experiments including

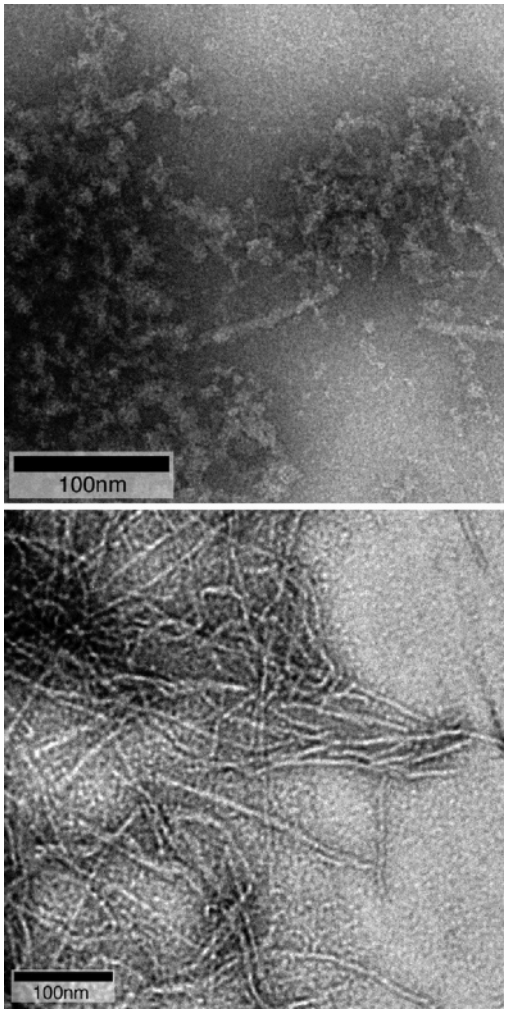

Figure 5. Representative negative stain TEM images. Peptide **5** (a) before heating as an amorphous α-helical aggregate and (b) after heating and conversion to β-sheet nanofibers. See Figure 3 of the Supporting Information for additional images.

transmission and grazing angle experiments. By orienting the peptide fibers with respect to the IR beam one can achieve a bias in the amide I versus amide II absorption. Examination of the bias allows one to determine the orientation of the amide bond and thus the orientation of the hydrogen-bonding network with respect to the nanofiber.[27,28] Attenuation of the amide I band with respect to the amide II band as seen in grazing angle FT-IR (Figure 4 of the Supporting Information) versus the transmission IR spectrum demonstrates that the hydrogen-bonding network is parallel to the fiber axis. Taken together, (1) the TEM demonstrates the nanofibrous nature of the self-assembled structure, (2) the IR demonstrates that the fiber is composed of β-sheets, and (3) oriented IR demonstrates that the β-sheet orientation is "cross-spine" in that the peptide backbone is perpendicular to the fiber axis (hydrogen-bonding network is parallel to the fiber axis) and therefore is consistent with the proposed characteristic structure of amyloid-like peptides

Two additional peptides were prepared to examine the importance of tyrosine as the β-sheet-inducing amino acid or if this is simply a hydrophobic effect. Peptides **7** and **8** replace tyrosine with phenylalanine and leucine, respectively. Both of these peptides were found to be even more prone to β-sheet formation. For example, the ATR FT-IR spectrum shows that even at room temperature a small fraction of peptide **7** converts to β-sheet upon drying for analysis. Drying results in a very

high peptide concentration, which drives the peptide toward the more thermodynamically stable β-sheet structure. Heating to 50 °C converts the majority of the peptide to the antiparallel β-sheet conformation as indicated by peaks at 1622 and 1692 cm^{-1} (Figure 4i). The presence of β-sheet in peptide **8** even at room temperature eliminates the lag time seen in other peptides, and conversion to β-sheet is complete in 4.0 min (Figure 3b). CD measurements correlated with the FT-IR data (Figures 4d and 4e).

Discussion

Recent studies on short peptides that can undergo conformational change from α to β structures have suggested two possible rationalizations for these mixed personalities. One suggests that the introduction of amino acids with a high propensity for β-sheet secondary structure in a sequence that is otherwise designed for α-helical character allows the second structural motif to become possible.[9,29] The other study[7] suggests that the key factor is instead the regular alternation between hydrophobic and hydrophilic amino acids. This alternation produces a facial amphiphile when the peptide is in the fully extended conformation that can be stabilized when two of these amphiphiles pack their hydrophobic faces against one another. Our work supports the alternating hydrophobic/hydrophilic model. Comparisons of peptide **1** with **3** and peptide **5** with **6** show that although the peptides have identical amino acid compositions and therefore identical secondary structural propensities the pattern of hydrophobic and hydrophilic amino acids has been altered favoring α-helices in the cases of peptides **3** and **6** and β-sheets in the cases of peptides **1** and **5**.

In situations in which hydrophobic and hydrophilic amino acids regularly alternate with one another a facial amphiphile is formed that is stabilized in the cross-beta fiber structure[10,30] observed in amyloids. In this fiber, hydrophobic amino acids can easily pack against one another, leaving hydrophilic amino acids on the exterior that can interact with water or form hydrogen bonds and/or salt bridges with additional peptide lamellae. In particular this theory is upheld by experiments in which the hydrophobic and hydrophilic amino acids in the c and f positions are swapped, leaving the peptides with identical amino acid compositions and only changing the hydrophobic/hydrophilic patterning. This type of alternation of hydrophobic and hydrophilic amino acids has previously been used to design synthetic amyloid-like nanofibers that are composed of regularly alternating hydrophobic and hydrophilic amino acids.[8,31]

Within the context of α-helical coiled coils, the f position in a heptad repeat is uniquely situated between the required hydrophobic amino acids in positions d and a such that mutation of this position to a hydrophobic amino acid clusters three contiguous hydrophobic amino acids on one face of the molecule when it is in an extended conformation. The fact that patterning of hydrophobic and hydrophilic amino acids plays such a large role in determining secondary structure should not be surprising since this is exactly how α-helical coiled coils are generated; the patterning of hydrophobic amino acids in the a and d positions, which can only be packed in an energetically favorable way within an α-helix, drives its formation regardless of the fact that these hydrophobic amino acids (Val, Ile, and Leu) have a high β-sheet propensity. Furthermore, recent studies of coiled coils have shown that nearly any hydrophobic amino acid is able to be substituted into these positions, including phenylalanine and hexafluoroleucine.[32,33] Incorporating a hydrophobic amino acid in the f position allows a second conformation, the β-sheet, to stabilize the hydrophobic d and a amino acids.

Considering the higher hydrophobicity of Phe and Leu as compared to Tyr,[34] a strengthened hydrophobic cluster should be created to direct the self-assembly of the peptides toward formation of β-sheet. Phenylalanine-containing peptide **7** has the minimum transition temperature required to accomplish conversion (Table 2), likely because not only is Phe highly hydrophobic but it also can have $\pi-\pi$ interaction between chains during peptide aggregation to β-sheets. Recently, many other studies have implicated aromatic interactions in the early stages of self-assembly of disease-related peptides[35,36] in terms of their ability to provide order and directionality within amyloid fibers. Other studies[37,38] specifically design peptides with a pair of Phe residues that may bind to the amyloid-like peptide, taking advantage of aromatic interaction between each other, such that amyloid formation was inhibited. The study presented here is consistent with these observations, although the sequences of peptides varies dramatically from the well-known amyloid-beta peptide. The peptide transition from α-helix to β-sheet and the helix-inducing ability shown by the Phe and Leu[39,40] residues justify our above statement that the structural conversion is not related to the introduction of amino acids with high β-sheet-forming propensity but rather the patterning of hydrophobic and hydrophilic amino acids. It has been believed that changing the amino acid in the f position does not affect the stability of the native helical structure as long as its sequence conforms to the general hydrophilic/hydrophobic profile of the heptad repeating pattern since they lie away from the hydrophobic core of coiled coils; however, in the course of our investigation, this tolerance of amino acid substitution on coiled coils was in fact limited due to the competition between α-helix and β-sheet structure.

Conclusion

In this paper we have prepared a series of short peptides that uniformly contain the canonical α-helical coiled-coil motif. These peptides can all adopt the α-helical conformation. However, when additional hydrophobic amino acids are incorporated into the non-interacting region of the coiled coil, in position f of the heptad, the peptides can convert to amyloid-like β-sheets. Moving this hydrophobic amino acid to the c position, another non-interacting portion of the coiled-coil, significantly reduces the rate at which this conversion takes place and indicates that the hydrophobic/hydrophilic alternating pattern that is established when f is hydrophobic is responsible for the structural polymorphism. This work helps to elucidate the mechanisms of structural polymorphism in amyloid-forming proteins and should help to guide the design of both coiled-coil and β-sheet peptide architectures.

Experimental Methods

Peptide Synthesis and Purification. Peptides were synthesized on an Advanced Chemtech Apex 396 peptide synthesizer using FMOC solid-phase chemistry with *O*-benzotriazole *N*,*N*,*N*′,*N*′- tetramethyl-uronium hexafluorophosphate (HBTU), 1-hydroxybenzotriazole hydrate (HoBt), and *N*,*N*-diisopropylethylamine (DIEA) as coupling reagents based on a 0.3 or 0.15 mmol scale. After completion of the peptide sequence, the peptide was acetylated in the presence of acetic anhydride and DIEA at a molar ratio of 8.3:1 in dichloromethane and then was cleaved and deprotected with a mixture of trifluoroacetic acid (TFA)/anisole/triisopropanolsilane/water (30:1:1:1 by volume). Purification of the peptides was carried out by reverse-phase high-performance liquid chromatography (HPLC) using a C-18 column with a linear gradient of acetonitrile and water containing 0.05% TFA. Matrix-assisted laser desorption ionization time-of-flight (MALDI-TOF) mass spectrometry was used to characterize the mass of the final products.

Peptide **1**, expected mass $[M + Na]^+$: 1757. Observed mass: 1757. Peptide **2**, expected mass $[M + Na]^+$: 1680. Observed mass: 1680. Peptide **3**, expected mass $[M + Na]^+$: 1757 Observed mass: 1758. Peptide **4**, expected mass $[M + Na]^+$: 2527. Observed mass: 2528. Peptide **5**, expected mass $[M + Na]^+$: 2563. Observed mass: 2564. Peptide **6**, expected mass $[M + Na]^+$: 2563. Observed mass: 2563. Peptide **7**, expected mass $[M + Na]^+$: 2531. Observed mass: 2532. Peptide **8**, expected mass $[M + Na]^+$: 2463. Observed mass: 2464. HPLC and mass spectrometry for peptides **2**, **3**, and **5**−**8** are shown in Figure 1 of the Supporting Information.

Circular Dichroism Spectroscopy. CD measurements were performed with a Jasco-J810 spectropolarimeter using quartz cells with 0.1 or 1 mm path lengths depending on sample concentration. Concentrations of peptides were calculated based on their absorption at 280 nm, except for peptide **2** due to the lack of aromatic residues in the sequence. Final concentrations of peptides **1**−**3** and peptides **4**−**8** were 0.8 and 0.4 mg/mL, respectively. In the cases of all peptides the pH was first adjusted to 10 to break up any aggregations and then adjusted by addition of 0.1 mM HCl until the desired value was obtained. CD spectra were recorded in millidegrees and converted to residual molar ellipticity. Thermal unfolding curves were obtained through an increase of 1 °C/min. Results of kinetics studies shown in Figure 3 are expressed as the fraction converted from α-helix to β-sheet secondary structure, which is calculated from $(\theta - \theta_{initial})/(\theta_{end} - \theta_{initial})$ where $\theta_{initial}$, θ_{end}, and θ represent the initial, final, and any-given time ellipticities monitored at 205 nm.

Analytical Ultracentrifugation. The apparent molar masses of peptides **1**, **3**, and **4** were determined in a Beckman Optical XL-A analytical ultracentrifuge equipped with a Ti60 titanium four-hole rotor with a six-channel and 12 mm path length centerpiece. Equilibrium experiments were performed at 5 or 20 °C using three different concentrations (peptides **1** and **3**, 0.17, 0.35, 0.56 mM; peptide **4**, 0.21, 0.42, 0.67 mM). Samples were run at three different rotor speeds: 50 000, 55 000 rpm, and 60 000 rpm. Loading volumes of the sample and reference were 95 and 110 μL, respectively. The sample was believed to be at equilibrium when the peptide distribution remained constant over 2 h at a given rotor speed (typically 14 h of rotation). Data analysis was carried out using a single-species model function by a nonlinear least-squares method provided by UltraScan software.[41] Calculated masses were as follows: Peptide **1** (pH = 3, 10 mM phosphate buffer, 5 °C): 3300. Peptide **3** (pH = 3, 10 mM phosphate buffer, 5 °C): 3149. Peptide **4** (pH = 4, 10 mM acetic acid buffer, 20 °C): 5369. Data for peptide **3** are shown in Figure 2 of the Supporting Information.

FT-IR Measurements. Peptide solutions were prepared as described for CD measurements. Aliquots of peptide sample were pipetted onto a diamond ATR crystal (Specac "Golden Gate"), CaF_2 window, or gold mirror, depending on the technique employed, dried under nitrogen, and examined using a Jasco FTIR 660plus. Concentrations of peptides **1**−**4** and **5**−**8** were 10 and 0.4 mg/mL, respectively. Grazing angle FT-IR spectra were recorded with a 80Spec specular reflectance accessory (PIKE Technologies).

Transmission Electron Microscopy. Peptide solutions were prepared as described for CD measurements. Approximately 15 μL of the peptide suspension was applied to a holey-carbon-coated copper grid (Quantifoil Cu 400 mesh R1.2/R1.3) for 30 s before wicking away excess solution. The sample on the grid was negatively stained with a 2% (w/v) phosphotungstic acid (adjusted to pH = 3 with NaOH) for 30 s. Excess stain solution was wicked off. Staining was repeated once. After complete drying, grids were examined by TEM at 200 kV (JEOL 2010 TEM).

Acknowledgment. We are grateful for the support of the Welch Foundation (Grant No. C-1557), the Nanoscale Interdisciplinary Research Team program of the National Science Foundation (Grant No. EEC-0304097), and the Multidisciplinary University Research Initiative of the Department of Defense (Grant No. W911NF-04-01-0203). J.D.H. is a recipient of the Searle Scholar Award.

Supporting Information Available. HPLC, mass spectrometry, oriented FT-IR, and analytical ultracentrifugation data. This material is available free of charge via the Internet at http://pubs.acs.org.

References and Notes

(1) Crick, F. H. C. *Acta Crystallogr.* **1953**, *6*, 689−697.
(2) McLachlan, A. D.; Stewart, M. *J. Mol. Biol.* **1975**, *98*, 293−304.
(3) O'Shea, E. K.; Rutkowski, R.; Kim, P. S. *Science* **1989**, *243*, 538−542.
(4) Serpell, L. C.; Blake, C. C. F.; Fraser, P. E. *Biochemistry* **2000**, *39*, 13269−13275.
(5) Hwang, W.; Zhang, S.; Kamm, R. D.; Karplus, M. *Proc. Natl. Acad. Sci. U.S.A.* **2004**, *101*, 12916−12921.
(6) Makin, O. S.; Atkins, E.; Sikorski, P.; Johansson, J.; Serpell, L. C. *Proc. Natl. Acad. Sci U.S.A.* **2005**, *102*, 315−320.
(7) Kammerer, R. A.; Kostrewa, D.; Zurdo, J.; Detken, A.; García-Echeverría, C.; Green, J. D.; Müller, S. A.; Meier, B. H.; Winkler, F. K.; Dobson, C. M.; Steinmetz, M. O. *Proc. Natl. Acad. Sci. U.S.A.* **2004**, *101*, 4435−4440.
(8) Lamm, M. S.; Rajagopal, K.; Schneider, J. P.; Pochan, D. J. *J. Am. Chem. Soc.* **2005**, *127*, 16692−16700.
(9) Pagel, K.; Wagner, S. C.; Samedov, K.; von Berlepsch, H.; Bottcher, C.; Koksch, B. *J. Am. Chem. Soc.* **2006**, *128*, 2196−2197.
(10) Luhrs, T.; Ritter, C.; Adrian, M.; Riek-Loher, D.; Bohrmann, B.; Dobeli, H.; Schubert, D.; Riek, R. *Proc. Natl. Acad. Sci. U.S.A.* **2005**, *102*, 17342−17347.
(11) DeGrado, W. F.; Lear, J. D. *J. Am. Chem. Soc* **1985**, *107*, 7684−7689.
(12) Mutter, M.; Hersperger, R. *Angew. Chem., Int. Ed.* **1990**, *29*, 185−187.
(13) Dado, G. P.; Gellman, S. H. *J. Am. Chem. Soc* **1993**, *115*, 12609−12610.
(14) Schenck, H. L.; Dado, G. P.; Gellman, S. H. *J. Am. Chem. Soc* **1996**, *118*, 12487−12494.
(15) Dzwolak, W.; Muraki, T.; Kato, M.; Taniguchi, Y. *Biopolymers* **2004**, *73*, 463−469.
(16) Pagel, K.; Vagt, T.; Kohajda, T.; Koksch, B. *Org. Biomol. Chem.* **2005**, *3*, 2500−2502.
(17) Cerasoli, E.; Sharpe, B. K.; Woolfson, D. N. *J. Am. Chem. Soc.* **2005**, *127*, 15008−15009.
(18) Takahashi, T.; Ueno, A.; Mihara, H. *Structure* **2000**, *8*, 915−925.
(19) Takahashi, T.; Yamashita, T.; Ueno, A.; Mihara, H. *Tetrahedron* **2000**, *56*, 7011−7018.
(20) Takahashi, T.; Ueno, A.; Mihara, H. *Bioorg. Med. Chem.* **1999**, *7*, 177−185.
(21) Takahashi, T.; Ueno, A.; Mihara, H. *Chem.—Eur. J* **1998**, *4*, 2475−2484.
(22) Zhang, S.; Rich, A. *Proc. Natl. Acad. Sci. U.S.A.* **1997**, *94*, 23−28.
(23) Altman, M.; Lee, P.; Rich, A.; Zhang, S. G. *Protein Sci.* **2000**, *9*, 1095−1105.
(24) Danielsson, J.; Jarvet, J.; Damberg, P.; Graeslund, A. *FEBS J.* **2005**, *272*, 3938−3949.
(25) Xu, Y.; Shen, J.; Luo, X.; Zhu, W.; Chen, K.; Ma, J.; Jiang, H. *Proc. Natl. Acad. Sci. U.S.A.* **2005**, *102*, 5403−5407.
(26) Dong, H.; Hartgerink, J. D. *Biomacromolecules* **2006**, *7*, 691−695.
(27) Paramonov, S. E.; Jun, H. W.; Hartgerink, J. D. *J. Am. Chem. Soc.* **2006**, *128*, 7291−7298.
(28) Kim, H. S.; Hartgerink, J. D.; Ghadiri, M. R. *J. Am. Chem. Soc.* **1998**, *120*, 4417−4424.
(29) Ciani, B.; Hutchinson, E. G.; Sessions, R. B.; Woolfson, D. N. *J. Biol. Chem.* **2002**, *277*, 10150−10155.
(30) Nelson, R.; Sawaya, M. R.; Balbirnie, M.; Madsen, A. O.; Riekel, C.; Grothe, R.; Eisenberg, D. *Nature* **2005**, *435*, 773−778.
(31) Yokoi, H.; Kinoshita, T.; Zhang, S. *Proc. Natl. Acad. Sci. U.S.A.* **2005**, *102*, 8414−8419.
(32) Bilgicer, B.; Fichera, A.; Kumar, K. *J. Am. Chem. Soc.* **2001**, *123*, 4393−4399.
(33) Yoder, N. C.; Kumar, K. *J. Am. Chem. Soc.* **2006**, *128*, 188−191.
(34) Black, S. D.; Mould, D. R. *Anal. Biochem.* **1991**, *191*, 72−82.
(35) Cohen, T.; Marom, A. F.; Rechter, M.; Gazit, E. *Biochemistry* **2006**, *45*, 4727−4735.
(36) Sato, T.; Campard-Kienlen, P.; Ahmed, M.; Liu, W.; Li, H.; Elliott, J. I.; Aimoto, S.; Constantinescu, S. N.; Octave, J. N.; Smith, S. O. *Biochemistry* **2006**, *45*, 5503−5516.

(37) Findeis, M. A.; Musso, G. M.; Arico-Muendel, C. C.; Benjamin, H. W.; Hundal, A. M.; Lee, J. J.; Chin, J.; Kelley, M.; Wakefield, J.; Hayward, N. J.; Molineaux, S. M. *Biochemisty* **1999**, *38*, 6791−6800.
(38) Cleary, J. P.; Walsh, D. M.; Hofmeister, J. J.; Shankar, G. M.; Kuskowski, M. A.; Seikoe, D. J.; Ashe, K. H. *Nat. Neurosci.* **2005**, *8*, 79−84.
(39) Willams, R. W.; Change, A.; Juretic, D.; Loughran, S. *Biochim. Biophys. Acta* **1987**, *916*, 200−204.
(40) O'Neil, K. T.; DeGrado, W. F. *Science* **1990**, *250*, 646−651.
(41) UltraScan II Home Page. http://www.ultrascan.uthscsa.edu, 2004.

BM060871M